Safe Reaction of a Robot Arm with Torque Sensing Ability on the External Disturbance and Impact: Implementation of a New Variable Impedance Control

Dzmitry Tsetserukou, Hiroyuki Kajimoto, Naoki Kawakami, Susumu Tachi

Abstract:

The paper focuses on control of a new anthropomorphic robot arm enabling the torque measurement in each joint to ensure safety while performing tasks of physical interaction with human and environment. A novel variable control strategy was elaborated to increase the robot functionality and to achieve human-like dynamics of interaction. The algorithm of impact control imparting reflex action ability to the robot arm was proposed. The experimental results showed successful recognition and realization of three different types of interaction: service task, co-operative task, and impact state.

Keywords: *human-robot interaction, anthropomorphic robot arm, variable impedance controller.*

1. Introduction

Many operations in specific environments (e.g. nuclear, in-space, underwater) are dangerous for human or difficult to access (e.g. micromanipulation, surgery). Recently, teleoperation is gaining increased attention by researchers interested in studying the possibilities to overcome the limited functionality of autonomous robots performing specific tasks, and to improve dexterous operations.

We successfully developed master-slave robot systems (TELESAR I and TELESAR II) based on the telexistence concept and gradually improved performance and stability of teleoperation [1]. The operator cockpit has two 6-DOF exoskeleton-type structure arms with hands. The slave robot enables to perform complex interaction with objects in environment by means of 7-DOF arms and 8-DOF hands. The contact tasks of a tip of the end-effector with environment are provided by impedance control algorithm. A slave robot controlled by the operator mainly performs the manipulations in unknown and unstructured human environment. The operator has to move the slave robot arm to target position, and to perform manipulations while simultaneously avoiding obstacles. However, operators cannot accomplish these tasks in real time. Besides, they are not perfect in planning the collision-free motion in dynamic unstructured surroundings. Recent researches on teleoperation are focusing on automation of collision avoidance and contact task based on information from sensors, allowing thus operator to concentrate on the task to be performed. The Robonaut teleoperated robot was developed to assist in-space operations and work with humans in space exploration [2]. The developed manipulator hand has very good force sensing ability due to the 6-axis force sensors attached at the fingertips and 19 Force Sensing Resistors. Using this force/tactile sensing ability, the operator moves the robot arm until the palm contacts an object, and then, grasping algorithm is activated. However, collision or expected contact with an environment may occur on the entire surface of the robot arm (e.g. forearm, elbow, upper arm, shoulder) producing interactive forces. Moreover, teleoperated robot in rescue and some other applications has to interact with human being in various co-operative tasks. In these fields, human-robot interaction represents a crucial factor for a robot design and imposes strict requirements on its behaviour and control in order to ensure safe interaction with environment and effectiveness while target task execution.

Several effective methods on enhancement of contact detection ability of manipulator were reported. To avoid collisions in time-varying environment, Lumelsky *et al.* [3] proposed to cover manipulator with a sensitive skin capable of detecting nearby objects. As this device integrates a huge amount of small sensors incorporated on a tiny rigid platform, and requires complicated wiring and signal processing hardware, such devices have high cost and reliability issues. Besides, sensitive skin provides only contact pattern information. Finding the technical solution for trade-off between safety and performance is the target of the new manipulation technology. To cope with this issue, the active compliance control implying fast joint torque controlling based on measuring the applied external torque in each joint was developed. The first embodiment of torque measurement is the integration of a torque sensor into each joint of the manipulator. The impedance control generates compliant trajectory based on measured external torque information. Such approach has two main advantages: (1) sensor detects not only forces applied to the hand but also those exerted at other points on the manipulator, (2) and allows to increase the performance for fast movements by active vibration dam-ping. Several attempts have been made by researchers to improve joint torque control. Wu and Paul [4] proposed simple, wide bandwidth, torque servo system using strain-gauge-based joint torque sensor. The developed torque-controlled lightweight robot arm with high load to weight ratio is described in [5]. Each joint of the arm is facilitated with strain-gauge-based torque sensor, posi-tion sensor and piezzo-brake. Sakaki and Iwakane [6] proposed to use a compact motor drive with embedded magnetostrictive torque sensor for impedance control of the robot arm. The approach of torque measurement through the elasticity of the harmonic drive flex-splines allows keeping the same stiffness and mechanical structure of the robot [7]. This method requires the strain

gauges to be installed on the flexsplines. The crucial shortcomings of the torque measurement approaches mentioned above are discussed in the paper [8]. The alternative method for increasing the safety level of robot arms interacting with humans is intentionally introducing compliance at the mechanical design level. The main idea is decoupling the rotor inertia from the link inertia through using passive elasticity [9]. However, the robot control is complicated by many unknown parameters (e.g. actuator stiffness and damping). Furthermore, compliant transmission negatively affects the performance in term of increased oscillations and settling time.

To realize the safe physical contact of entire robot arm structure with human and to guarantee the collision avoidance, our primary idea is concentrated on the design of a whole-sensitive robot arm (by using distributed optical torque sensors in each joint). When contact with environment occurs, manipulator automatically adjusts its dynamic parameters (stiffness and damping) according to the measured external torque and time derivative of torque. The newly developed anthropomorphic manipulator iSoRA (**i**ntelligent **So**ft **R**obot **A**rm) having 4-DOF arm and 8-DOF hand (Fig. 1) is capable to safely interact with environment wherever contact occurs on the arm surface.
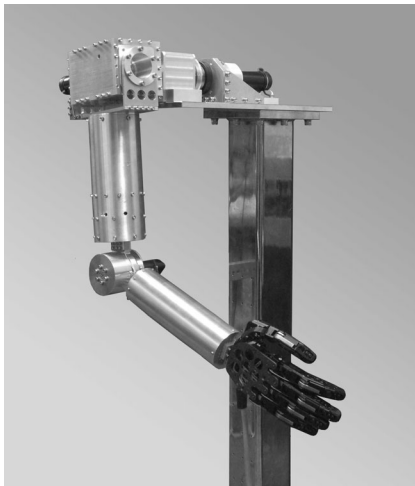

Fig. 1. iSoRA robot arm.

The distinctive features of our approach are as follows:
1) We use optical approach for torque measurement, which allows avoiding inherent shortcomings of strain-gauge-based and magnetostrictive force/torque sensors. We developed new optical torque sensors having high dependability, good accuracy (even in electrically noisy environment), low price, compact sizes, and easy manufacturing and calibration procedure [8].
2) The stiffness of the proposed sensor is much smaller then previously proposed. So, when collision takes place, the injuries of human can be considerably reduced through compliant coupling between the motor rotor inertia and the link inertia.
3) The intelligent variable impedance control and reflex-action-based impact control were elaborated to realize safe, smooth and natural human-robot interaction.

The remainder of the paper is structured as follows.

Section 2 describes the development of a whole-sensitive robot arm. The elaborated intelligent variable impedance control algorithm allowing contact state recognition and the experimental results are discussed in Section 3. In Section 4, we briefly conclude the paper.

2. Design of a new anthropomorphic robot arm

From the safety point of view, to minimize injures in case of collision, most of the robot parts were manufactured from aluminium alloys to obtain as much lightweight structure as possible. The robot links were designed in round shape to reduce impact force. The distribution of the arm joints replicates the human arm structure in order to make it easy to operate using kinaesthetic sensation during teleoperation. To remove mechanical subsystems without disassembling the main structure when the failures do occur, we have been using a modular approach while designing anthropomorphic robot arm. Therefore, we selected CSF-series gear head type of Harmonic Drive instead of compact and lightweight component one. The Harmonic Drive offers such advantages as accurate positioning, high torque capability, torsional stiffness, and high single stage ratios. Developed robot arm has 4-DOF: Roll, Pitch, Yaw joints of a shoulder, and Pitch joint of an elbow. Each joint is equipped with optical torque sensor directly connected to the output shaft of Harmonic Drive. The sizes and appearance of the arm were chosen so that the sense of incongruity during interaction with human is avoided. We kept the arm proportions the same as in average height human: upper arm length L_1 of 0.308 m; upper arm circumference of 0.251 m (diameter 0.080 m); forearm length L_2 of 0.241 m; forearm circumference of 0.189 m (diameter 0.06 m). The 3D CAD model of the developed arm and coordinate systems based on Denavit-Harten-berg convention are represented in Fig. 2.
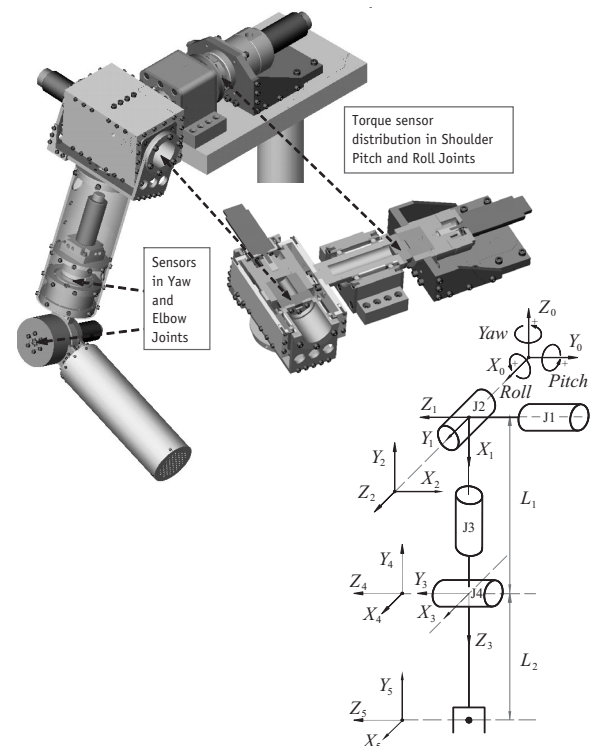

Fig. 2. 3D CAD model and coordinate systems.

The motors are equipped with magnetic encoders having 512 pulses per revolution. To protect the sensor against influence of bending moment and axial force, the simple supported loaded shaft configuration was implemented using two sets of bearings. The principal specifications of the developed arm and kinematic parameter values are given in Table 1 and Table 2, respectively.

Table 1. Principal specifications.

Parameters	Arm joints			
	Shoulder			Elbow
	J1, Pitch	J2, Roll	J3, Yaw	J4, Pitch
Mobility range (New robot arm/ Human arm) [deg]	-180 to 180 (-60 to 180)	-180 to10 (-165 to 0)	-180 to 180 (-60 to 180)	0 to 112 (0 to 130)
Motor power [W], motor type	90, Maxon RE 35	60, Maxon RE 35	26.6, Faulhaber 2657	26.6, Faulhaber 2657
Harmonic drive rated torque [Nm], (type/ gear ratio)	7.8, (CSF-14-GH /100)	7.8, (CSF-14-GH /100)	5.0, (CSF-11-2XH/100)	5.0, (CSF-11-2XH/100)

Table 2. Denavit-Hartenberg parameters.

i	α_{i-1} [deg]	a_{i-1} [m]	d_i [m]	θ_i [deg]
1	90	0	0	θ_1-90
2	-90	0	0	θ_2+90
3	90	0	L_1	θ_3+90
4	-90	0	0	θ_4-90
5	0	L_2	0	0

3. The impedance control

3.1. Joint impedance control

The dynamic equation of an *n*-DOF manipulator in joint space coordinates (during interaction with environment) is given by:

$$M(\theta)\ddot{\theta} + C(\theta,\dot{\theta})\dot{\theta} + \tau_f(\dot{\theta}) + g(\theta) = \tau + \tau_{EXT}, \quad (1)$$

where $\theta, \dot{\theta}, \ddot{\theta}$ are the joint angle, the joint angular velocity, and the joint angle acceleration, respectively; $M(\theta) \in R^{n \times n}$ is the symmetric positive definite inertia matrix; $C(\theta,\dot{\theta}) \in R^n$ is the vector of Coriolis and centrifugal torques; $\tau_f(\dot{\theta}) \in R^n$ is the vector of actuator joint friction forces; $g(\theta) \in R^n$ is the vector of gravitational torques; $\tau \in R^n$ is the vector of actuator joint torques; $\tau_{EXT} \in R^n$ is the vector of external disturbance joint torques.

People can perform dexterous contact tasks in daily activities while regulating own dynamics according to time-varying environment. To achieve skilful human-like behaviour, the robot has to be able to change its dynamic characteristics depending on time-varying interaction forces. The most efficient method of controlling the interaction between a manipulator and an environment is impedance control. This approach enables to regulate response properties of the robot to external forces through modifying the mechanical impedance parame-

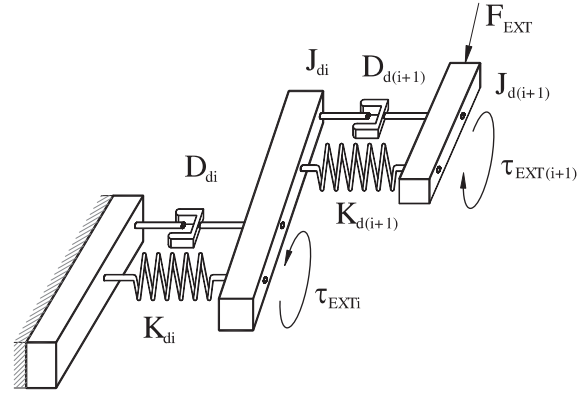ters. The graphical representation of joint impedance control is given in Fig. 3.

Fig. 3. Concept of the local impedance control.

The desired impedance properties of i-th joint of manipulator can be expressed as:

$$J_{di}\Delta\ddot{\theta}_i + D_{di}\Delta\dot{\theta}_i + K_{di}\Delta\theta_i = \tau_{EXTi}; \; \Delta\theta_i = \theta_{ci} - \theta_{di}, \quad (2)$$

where J_{di}, D_{di}, K_{di} are the desired inertia, damping, and stiffness of i-th joint, respectively; τ_{EXTi} is torque applied to i-th joint and caused by external and gravity forces, $\Delta\theta_i$ is the difference between the current position θ_{ci} and desired one θ_{di}. The state-space presentation of the equation of local impedance control is written as follows:

$$\begin{bmatrix} \Delta\dot{\theta}_i \\ \dot{v}_i \end{bmatrix} = \begin{bmatrix} 0 & 1 \\ -K_d/J_d & -D_d/J_d \end{bmatrix} \begin{bmatrix} \theta_i \\ v_i \end{bmatrix} + \begin{bmatrix} 0 \\ 1/J_d \end{bmatrix} \tau_{EXTi}(t), (3)$$

or:

$$\begin{bmatrix} \Delta\dot{\theta}_i \\ \dot{v}_i \end{bmatrix} = A \begin{bmatrix} \theta_i \\ v_i \end{bmatrix} + B\tau_{EXTi}(t), \quad (4)$$

where the state variable is defined as $v_i = \Delta\dot{\theta}_i$; A, B - matrices. After integration of (4), the discrete time presentation of the impedance equation is expressed as:

$$\begin{bmatrix} \Delta\theta_{k+1} \\ \Delta\dot{\theta}_{k+1} \end{bmatrix} = A_d \begin{bmatrix} \Delta\theta_k \\ \Delta\dot{\theta}_k \end{bmatrix} + B_d T_{EXT(k)}. \quad (5)$$

To achieve the fastest possible non-oscillatory response to the external force, we assigned the eigenvalues λ_1 and λ_2 of matrix A as real and equal $\lambda_1=\lambda_2=\lambda$, $\lambda>0$. By using Cayley-Hamilton method for matrix exponential determination, we have:

$$A_d = e^{\lambda T} \begin{bmatrix} 1-\lambda T & T \\ -K_d T/J_d & 1-\lambda T-D_d T/J_d \end{bmatrix}, \quad (6)$$

$$B_d = (A_d - I)A^{-1}B = -\frac{1}{K_d} \begin{bmatrix} e^{\lambda T}(1-\lambda T)-1 \\ -(D_d/(2J_d))^2 Te^{\lambda T} \end{bmatrix}, \quad (7)$$

where T is the sampling time; I is the identity matrix.

There are several conflicting requirements on the

choice of dynamics parameters of impedance model to provide effectiveness and functionality of robot in tasks of physical interactions fulfilled in co-operation with humans, and to ensure the collision avoidance. For example, while accomplishing service tasks for human in the autonomous mode, it is required to provide high stiffness (to ensure small position error during object handling) and high damping (for good velocity tracking). Realization of human following motion, mainly used in performing of co-operating tasks, also imposes specific requirements on desired impedance parameter selection. In this approach, by applying force to the robot arm, it is possible to intuitively operate the robot along the force and speed direction without considering any command signals. In the case of collision, the very small stiffness is obligatory to reduce the impact forces.

Basically, there are two types of solution of this problem: adaptive and functional adjustments of impedance parameters. In the adaptive control, damping and stiffness of the system are gradually adjusted according to sensed dynamics and contact forces [10]. However, due to parametric uncertainties of the robot dynamics model, it is difficult to obtain the complete description of the dynamics. Therefore, model-based adaptive impedance control must rely on either repeated motions or time for adaptation to achieve convergence to the desired system parameters. For systems with more then one DOF, such approach hardly can be applied. In the functional approaches, current impedance parameters have predetermined relations to the current sensed variables. Generally, these methods presume determining the current stiffness and damping matrices functionally dependent on sensed variables. The main idea of the paper [11] is that the involving contact between slave robot and the environment can be classified according to the angle between commanded velocity and the contact force. It is supposed that force and velocity vectors are usually parallel when the impact occurs or when the object is being pushed. So, the functional dependency of stiffness and damping on angle between sensed force and velocity vectors was proposed. In real co-operation tasks and, especially, collisions, these vectors can not only be parallel, but also have indepenent arbitrary directions according to external force coming direction.

Another line of variable impedance research is directed to estimation of human arm stiffness [12]. The proposed variable impedance controller varies a damping parameter of target impedance in proportion to an estimated value of the human arm stiffness. Despite the fact that robot can effectively follow the human arm motion, it cannot perform task autonomously. Besides, only impedance parameters of the robot end-effector can be adjusted. We elaborated a new methodology for impedance parameter adjustment based on the interaction mode and providing the dynamic stability of the system.

3.2. Intelligent variable joint impedance control

3.2.1. *Control of service task and human following motion*

The research on impedance characteristics of human arm shows that, while pushing or pulling the object naturally, human arm stiffness and damping behaviour can be approximated by exponential curves [13]. The first essential peculiarity of new control method is that we introduce the exponential functional dependency between sensed force and stiffness to impart the human-like damping and stiffness behaviour to the robot arm interacting with environment. The second main feature originates from the fundamental conflict in impedance selection with regard to current working conditions. We consider the threshold of external disturbance torque value τ_{EXTth} to distinct the service task (with high stiffness and damping of joints) from human following motion tasks requiring low stiffness. This value can be chosen depending on the force necessary to accomplish the service task. We assigned the specific magnitude of τ_{EXTth} to each joint of robot arm. The third distinctive contribution is the recognition of the collision based on the time derivative of joint torque. The procedure of impedance parameters selection is illustrated by the example of elbow joint as follows. On the first stage, the parameters of desirable impedance model of robot are computed for the case of service task accomplishment and average-level-contact-force of human-robot interaction. The desired stiffness K_{d1} (for static equilibrium case) is calculated from Eq. (8) based on the maximum deflection value of joint angle $\Delta\theta_{max}$ caused by external torque τ_{EXT} while service task performance.

$$K_{d1} = \frac{\tau_{EXT}}{\Delta\theta_{max}} \qquad (8)$$

It was defined that external torque of 1 Nm results in $\Delta\theta_{imax}$ of 0.1 rad giving the K_{d1} of 10 (Nm/rad). The desired damping is expressed as:

$$D_{d1} = 2\zeta\sqrt{K_{d1}J_{d1}} \qquad (9)$$

To realize fast non-oscillatory response on the external torque, we defined damping coefficient ζ of 1.05. The value of desired inertia J_{d1} of 0.1 (kg·m²) was assigned to realize fast response tracking. Thus, the value D_{d1} of 2.1 (Nm·s/rad) was derived from (9). These parameters are valid till the interaction force does not cause the overload of robot arm. When sensed value of the torque is larger then threshold level, robot recognizes this condition as human following motion mode, and adjusts its dynamics parameters (stiffness and damping) in the same way as humans in order to provide smooth natural interaction. To realize such continuous change of dynamics, we are using exponential relation between external disturbance torque and desired stiffness:

$$K_{d2} = K_{d1}e^{\mu(\tau_{EXT}-\tau_{EXTth})}, \qquad (10)$$

where K_{d2} is the desired stiffness on the second stage of interaction; μ is the coefficient defining the level of decreasing of arm joint stiffness in response on increasing difference between external torque and threshold external torque value. The desired damping is adjusted to prevent force responses from being too sluggish while changing stiffness values, and to ensure contact stability:

$$D_{d2} = 2.1\sqrt{K_{d2}J_{d1}} = 2.1e^{0.5\mu(\tau_{EXT}-\tau_{EXTth})}\sqrt{K_{d1}J_{d1}} \qquad (11)$$

Then, variable joint impedance controller is described by:

$$\mathrm{J}_{di}\Delta\ddot{\theta}_i + 2.1e^{0.5\mu(\tau_{EXTi}-\tau_{EXTth})}\sqrt{\mathrm{K}_{d1}\mathrm{J}_{d1}}\Delta\dot{\theta}_i +$$

$$+ \mathrm{K}_{d1}e^{\mu(\tau_{EXTi}-\tau_{EXTth})}\Delta\theta_i = \tau_{EXTi}; \ \Delta\theta_i = \theta_{ci} - \theta_{di} \qquad (12)$$

To verify the theory and to evaluate the feasibility and performance of the proposed impedance controller, the experiment with new whole sensitive robot arm was conducted. To ensure the effectiveness of service task accomplishment, we decided to implement position-based impedance control (Fig. 4). In this algorithm, compliant trajectory generated by the impedance controller is tracked by the PD control loop.

During the experiment, the interaction with arm was performed to exceed join torque threshold level (τ_{EXTth} of 0.6 Nm was assigned, $\mu = -1.155$). The experimental results for the elbow joint – applied torque, impedance trajectories with constant and variable coefficients, variable stiffness plot, variable damping plot, applied torque with different magnitudes and corresponding impedance trajectories with constant and variable coefficients – are presented in Fig. 5, Fig. 6, Fig. 7, Fig. 8, Fig. 9, and Fig. 10, respectively.

The experimental results show the successful realization of the variable joint impedance control. While contact with human, the robot arm generates compliant soft motion according to the sensed force. The plot presented in Fig. 6 shows that the variable impedance control
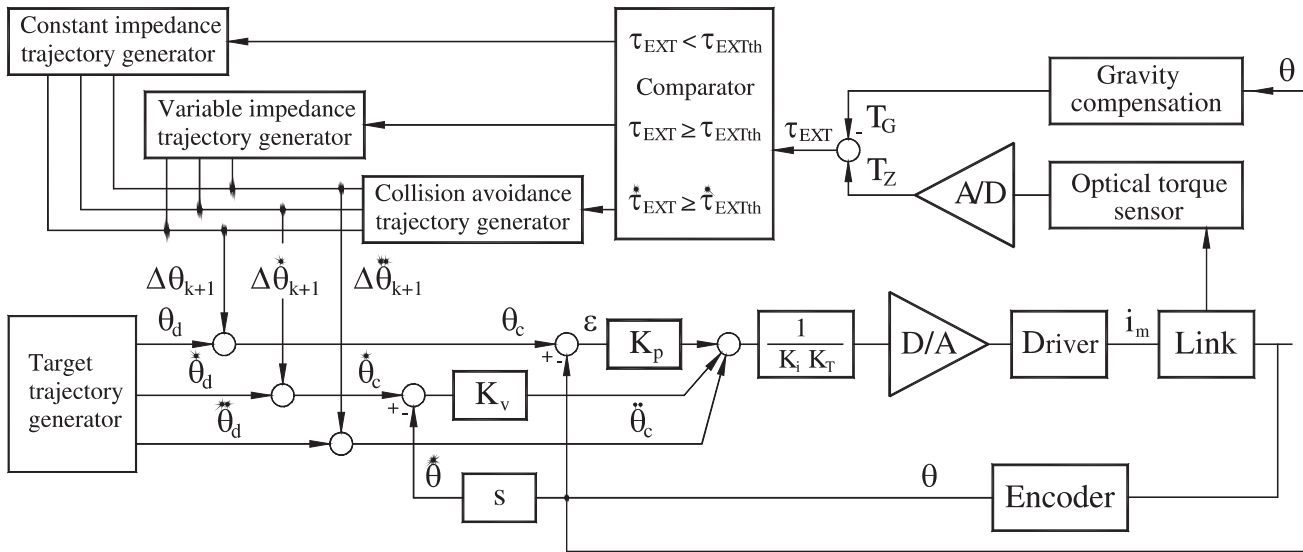

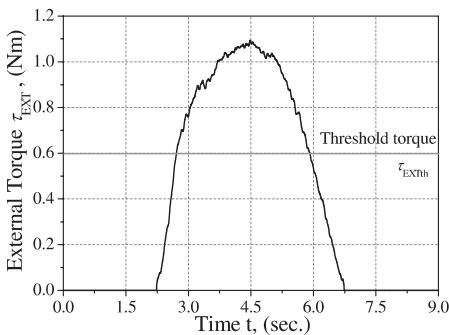Fig. 4. Block diagram of position-based impedance control.
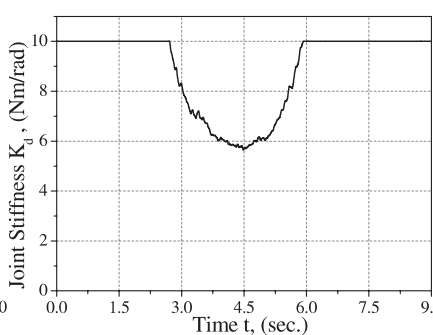

Fig. 5. External torque.

Fig. 7. Variable stiffness K_d.

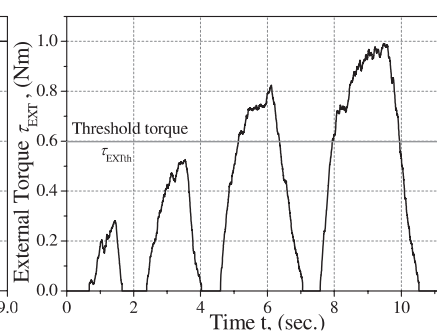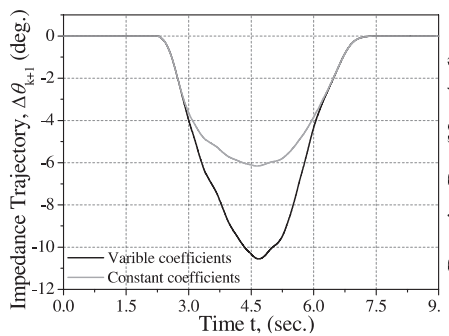Fig. 9. External torque.

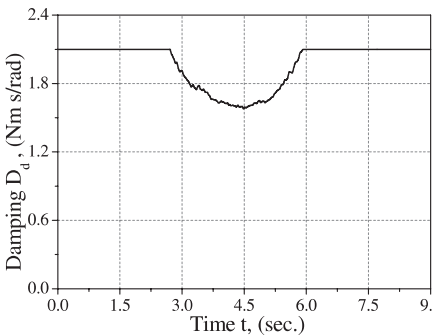Fig. 6. Impedance trajectories.
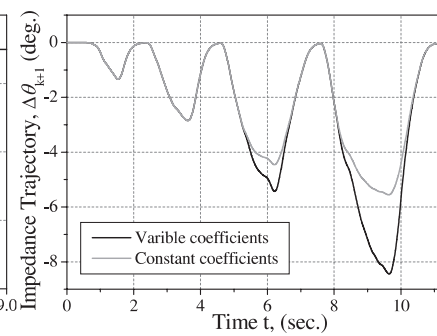

Fig. 8. Variable damping D_d.

Fig. 10. Impedance trajectories.

provides softer trajectory to accomplish human following motion than the impedance control with constant coefficients. As we assigned the critically damped response of impedance model to disturbance force, output angle $(\Delta\theta_{k+1})$ has ascending-descending exponential trajectory. As seen from the experimental results shown in Fig. 9 and Fig. 10, the proposed variable impedance control comprehensively distinguishes and processes the service tasks (torques under threshold level) and co-operative human following tasks (torques above threshold level).

As the result of the experiments with variable impedance-controlled arm, tactile sensation of soft friendly interaction was really achieved.

3.2.2. Impact control

In daily life, a person frequently contacts with an environment. The impact between a limb and environment is inevitable during interaction. In order to work in human daily environment, robot has to recognize the collision condition, and its control system should be able to quickly and smoothly guide manipulator to avoid excessively large impact force. Different impact control algorithms were proposed. Basically, they are focusing on preparing for impact in advance [14] and coping with impact during contact transience [15]. However, due to unexpected nature of collision and lack of the robust control strategy of impact effect minimization, the application area of such approaches is highly limited.

We believe that realization of the robust impact control should originate from human reflex system. A reflex action is an automatic involuntary neuromuscular action elicited by a defined stimulus, and it can respond to external stimuli with small reaction time retracting the limbs away from the object. In our control algorithm, impact is processed as follows. When an unexpected collision is detected, the impact control algorithm provides the pre-programmed reflex action of the robot arm. After accomplishment of a safe and smooth collision, the control system is returned to the original mode aimed at distinguishing the service and co-operating tasks.

While analysing the results of collision experiments, we came to conclusion that the large contact forces, mainly used as criterion of collision, do not indicate the impact, while the time derivative of force value does. In the developed impact control system, the value of the time derivative of torque $\dot{\tau}_{EXTth}$ exceeding the assigned threshold is inter-preted as collision state. To realize reflexive human-like behaviour, the stiffness of the impedance model of the robot arm on the first stage of contact transient has to be reduced drastically. Hence, exponential relation between time derivative of external torque and desired stiffness coefficient K_{d3} was defined with large coefficient μ of 0.7:

$$K_{d3} = K_{d1}e^{-\mu\dot{\tau}_{EXTth}} \tag{13}$$

To attenuate the oscillations of the robot arm, which are inherent to collision, the larger constant damping coefficient ζ of 1.25 was assigned. The value of desired damping coefficient is calculated from Eq. (9). In the second stage of contact transient, while time derivative of torque is negative, the high damping value reducing arm inertia effect is desired. For this case, the following relation between desired damping D_{d3} and time derivative of torque was specified:

$$D_{d3} = 2.5\sqrt{K_{d1}J_{d1}} - \alpha_d\dot{\tau} , \tag{14}$$

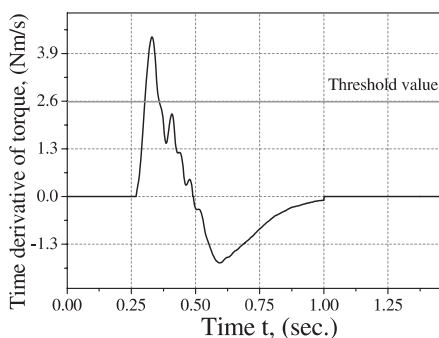where α_d is the weighting factor for damping (equals to 1.2).
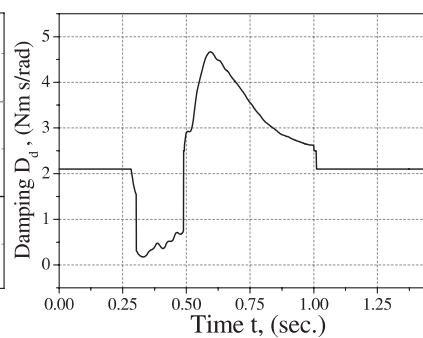

Fig. 11. Torque derivation.
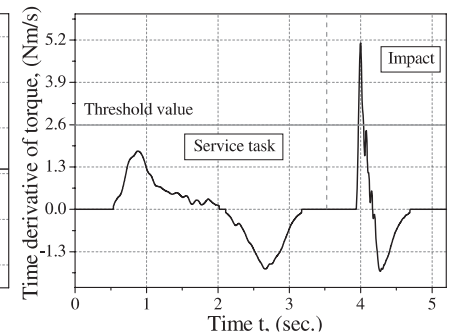

Fig. 13. Variable damping D_d.
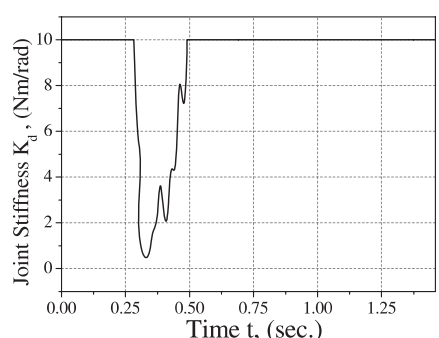

Fig. 15. Torque derivation.

Fig. 12. Variable stiffness.

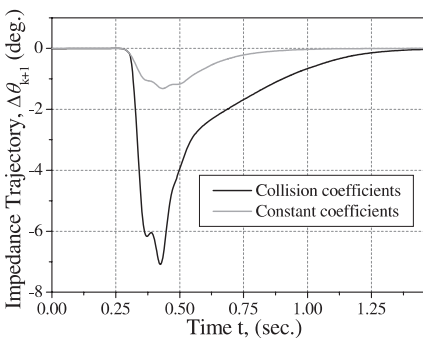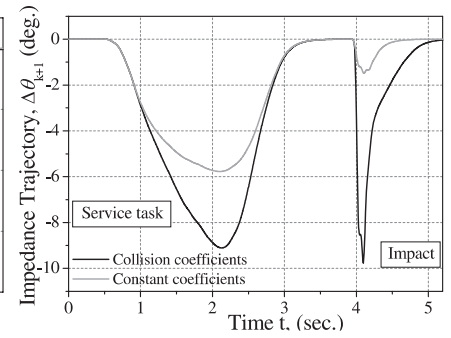Fig. 14. Impedance trajectories.

Fig. 16. Impedance trajectories.

The threshold value of the time derivative of torque $\dot{\tau}_{EXTth}$ was assigned to 2.6 Nm/s. The experimental results for the elbow joint – time derivative of applied torque, desired collision stiffness K_{d3}, desired collision damping D_{d3} plot, impedance trajectories with constant and collision variable coefficients, time derivative of torque for two different contact states and corresponding impedance trajectories – are presented in Fig. 11, Fig. 12, Fig. 13, Fig. 14, Fig. 15, and Fig. 16, respectively.

From the plots of experimental results, it is apparent that, when impact is recognized (time derivative of torque becomes larger than threshold value), the stiffness and damping are decreasing drastically (Fig. 12, Fig. 13), allowing avoidance of large impact forces. On the second stage of interaction, when the impact force is decreasing, the damping coefficient of impedance model (Fig. 13) is increased to suppress the dynamic oscillations. The Fig. 15 indicates that nature of co-operation tasks (time derivative of torque has small and stretched in time scale value) completely differs from impact state (time derivative of torque has large spike and is shortened in time scale value). The developed control takes advantage of this feature to generate reflex-action-based motion.

4. Conclusion

New whole-sensitive robot arm iSoRA was developed to provide human-like capabilities of contact task performing in a broad variety of environments. Each joint was facilitated with high-performance optical torque sensor. The intelligent variable impedance control and reflex-action-based impact control were elaborated to realize safe, smooth, and natural human-robot interaction. We introduced the exponential functional dependency between sensed force and stiffness to impart human-like damping and stiffness behavior to the robot arm. Experimental results of impact revealed that large contact forces, mainly used as criterion of collision, do not indicate the impact state, while the time derivative of force value does. The magnitude of time derivative of torque was used as an indicator of collision state. To realize reflexive human-like behavior, stiffness of the impedance model of robot arm was reduced drastically during collision transient. This was achieved by means of reciprocal functional dependency of stiffness on the value of time derivative of torque.

The conventionally impedance-controlled robot can provide contacting task only at the tip of the end-effector with predetermined dynamics. By contrast, approaches developed by us provide delicate continuous safe interaction of all surface of the arm with environment.

AUTHORS
Dzmitry Tsetserukou, Naoki Kawakami and Susumu Tachi - Department of Information Physics and Computing, The University of Tokyo, Japan. E-mails:
dima_teterukov@ipc.i.u-tokyo.ac.jp,
kawakami@star.t.u-tokyo.ac.jp,
tachi@star.t.u-tokyo.ac.jp.
Hiroyuki Kajimoto - Professor at Department of Human Communication, The Universityof Electro-Communications, Japan. E-mail: kajimoto@hc.uec.ac.jp.

References

[1] Tadakuma R., Asahara Y., Kajimoto H., Kawakami N., and Tachi S., "Development of anthropomorphic multi-D.O.F. master-slave arm for mutual telexistence," *IEEE Trans. Visualization and Computer Graphics*, vol. 11, Nov. 2005, no. 6, pp. 626-636.

[2] Diftler M.A., Culbert C. J., Ambrose R. O., Platt Jr. R., and Bluethmann W. J., "Evolution of the NASA/DARPA Robonaut control system". In: *Proc. 2003 IEEE Int. Conf. Robotics and Automation*, Taipei, 2003, pp. 2543-2548.

[3] Lumelsky V. J. and Cheung E., "Real-time collision avoidance in teleoperated whole-sensitive robot arm manipulators," *IEEE Trans. Systems, Man, and Cybernetics*, vol. 23, 1993, no. 1, pp. 194-203.

[4] C. H. Wu, Paul R. P., "Manipulator compliance based on joint torque control". In: *Proc. 19th IEEE Conf. Decision and Control,* Alberquerque, NM, 1980, pp. 88-94.

[5] Hirzinger G., Albu-Schaffer A., Hahnle M., Schaefer I., and Sporer N., "On a new generation of torque controlled light-weight robots". In: *Proc. 2001 IEEE Int. Conf. Robotics and Automation*, Seoul, Korea, 2001, pp. 3356-3363.

[6] Sakaki T., Iwakane T., "Impedance control of a manipulator using torque-controlled lightweight actuators", *IEEE Trans. Industry Applications*, vol. 28, Nov. 1992, no. 6, pp. 1399-1405.

[7] Hashimoto M., Kiyosawa Y., Paul R. P., "A torque sensing technique for robots with harmonic drives", *IEEE Trans. on Robotics and Automation*, vol. 9, Feb. 1993, no. 1, pp. 108-116.

[8] Tsetserukou D., Tadakuma R., Kajimoto H., Tachi S., "Optical torque sensors for implementation of local impedance control of the arm of humanoid robot". In: *Proc. 2006 IEEE Int. Conf. Robotics and Automation*, Orlando, 2006, pp. 1674-1679.

[9] Bicchi A., Tonietti G., "Fast and soft arm tactics: dealing with the safety-performance trade-off in robot arms design and control", *IEEE Robotics and Automation Magazine*, vol. 11, June 2004, no. 2, pp. 22-33.

[10] Carelli R., Kelly R., "Adaptive impedance/force controller for robot manipulators," *IEEE Trans. Automatic Control*, vol. 36, Aug. 1991, no. 8, pp. 967-972.

[11] Dubey R. V., Chang T. F., Everett S. E., "Variable damping impedance control of a bilateral telerobotic system", *IEEE Control Systems Magazine*, vol. 17, Feb. 1997, pp. 37-44.

[12] Tsumugiwa T., Yokogawa R., Hara K., "Variable impedance control based on estimation of human arm stiffness for human-robot cooperative calligraphic task". In: *Proc. 2002 IEEE Int. Conf. Robotics and Automation*, Washington DC, 2002, pp. 644-650.

[13] Rahman M. M., Ikeura R., Muzutani K., "Investigating the impedance characteristics of human arm for development of robot to cooperate with human operators", In: *Proc. 1999 IEEE International Conference Systems, Man and Cybernetics*, Tokyo, Japan, 1999, pp. 676-681.

[14] Walker I. D., "Impact configuration and measures for kinematically redundant and multiple armed robot system", *IEEE Trans. Robotics and Automation*, vol. 10, Oct. 1994, no. 5, pp. 670-683.

[15] Volpe R., Khosla P., "A theoretical and experimental investigation of impact control for manipulators", *Int. Journal of Robotics Research*, vol. 12, Aug.1993, no. 4, pp. 351-365.